Brain shift analysis for deep brain stimulation surgery using non-rigid registration

Muhammad F. Khan[a], Klaus Mewes[b], Robert Gross[c] and Oskar Škrinjar[a,d]

[a]School of Electrical and Computer Engineering, Georgia Institute of Technology, Atlanta, USA;
[b]Department of Neurology, School of Medicine, Emory University, Atlanta, USA;
[c]Department of Neurological Surgery, School of Medicine, Emory University, Atlanta, USA;
[d]Department of Biomedical Engineering, Georgia Institute of Technology, Atlanta, USA

ABSTRACT

Deep brain stimulation (DBS) surgery is a treatment for patients suffering from Parkinson's disease and other movement disorders. The success of the procedure depends on the implantation accuracy of the DBS electrode array. Surgical planning and navigation are done based on the pre-operative patient scans, assuming that brain tissues do not move from the time of the pre-operative image acquisition to the time of the surgery. We performed brain shift analysis on nine patients that underwent DBS surgery using a 3D non-rigid registration algorithm. The registration algorithm automatically aligns the pre-operative and the post-operative 3D MRI scans and provides the shift vectors over the entire brain. The images were first aligned rigidly and then non-rigidly registered with an algorithm based on thin plate splines and maximization of the normalized mutual information. Brain shift of up to 8 mm was recorded in the nine subjects, which is significant given that the size of the targets in the DBS surgery is a few millimeters.

Keywords: Brain shift, brain deformation, image registration, deep brain stimulation surgery

1. INTRODUCTION

DBS surgery, a type of microelectrode-guided surgery, is a recent and effective treatment for movement disorders including Parkinson's disease (PD), essential tremor, and dystonia.[1–5] It is an option for people whose disabling symptoms can no longer be controlled by medication. PD, marked by bradykinesia, muscular rigidity and resting tremor, is a progressive neurological disorder caused by a loss of nerve cells in the substantia nigra, a small area deep within the midbrain.[6] The cells that die are both inhibitory (indirect pathway) and excitatory (direct pathway) in the striatum. They produce dopamine, a chemical used to help direct muscle activity. Several forms of dystonia are believed to be associated with an imbalance of dopamine.[7] To date, the exact cause of PD is not known and there are no cures for PD, only means to reduce symptoms. Possible treatment options are drug-based (e.g. dopamine replacement), stereotactic neurosurgery,[8,9] and physical therapy.

DBS surgery is a stereotactic procedure that uses a permanently implanted electrode lead to deliver continuous high-frequency electrical stimulation to the ventral intermediate nucleus (Vim) of the thalamus (effective for tremor only), globus pallidus internus (GPi), or subthalamic nucleus (STN).[10,11] The exact mechanism of action is not yet known, but it is believed that high frequency stimulation in these areas modulates neuronal activity, helping to rebalance control messages throughout the movement control centers in the brain. This in turn causes improvements in the tremor, muscular rigidity and bradykinesia. The electrode is connected subcutaneously to a pacemaker-like device implanted below the collarbone. The success of the DBS surgery is mainly dependent upon the implantation accuracy of the deep brain stimulator at the target; Vim, STN or GPi.[12] The small size, surrounding neuronal structures, and fibre tracts make STN and GPi a difficult stereotactic target.[13] Since STN and GPi are not clearly visible in common imaging modalities, atlas-based techniques are used to help infer the target location. Most of the planning and preparation is done on the pre-operative (pre-op) scans (MRI or CT), and it is usually assumed that anatomical structures do not move between the pre-op image acquisition time and

Send correspondence to O.S.: E-mail: oskar.skrinjar@bme.gatech.edu

Medical Imaging 2007: Visualization and Image-Guided Procedures, edited by Kevin R. Cleary, Michael I. Miga,
Proc. of SPIE Vol. 6509, 65091B, (2007) · 1605-7422/07/$18 · doi: 10.1117/12.710009

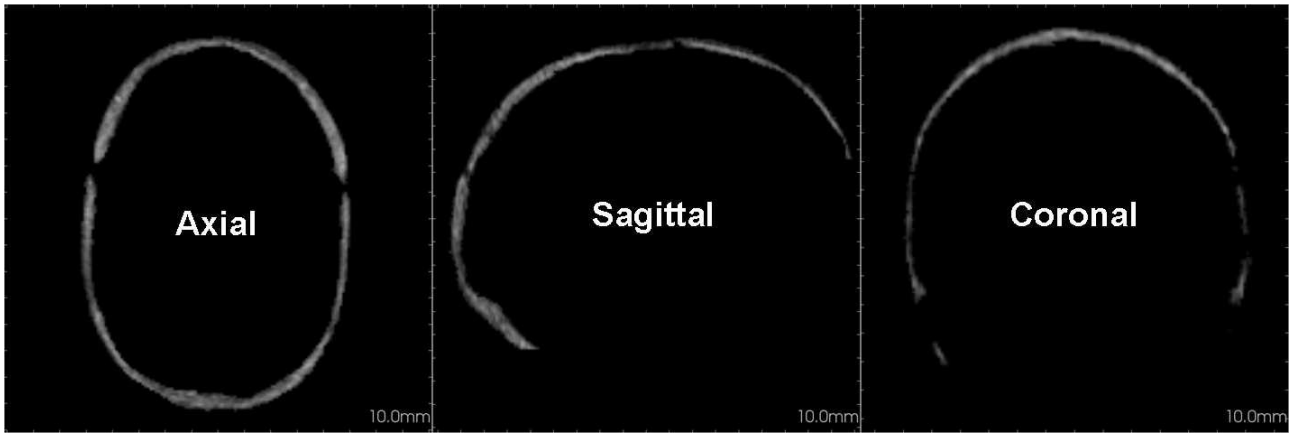

Figure 1. Axial, sagittal and coronal slices of the segmented diploë of one of the subjects.

the time of the surgery. However, some recent studies suggest that brain tissues shift during the surgery.[14,15] This movement of the brain may be due to one or more factors including: loss of cerebrospinal fluid (CSF), gravitational force, change in pressure due to skull opening during the surgery, pneumocephalus, and forces due to insertion of the DBS lead.

Microelectrode mapping can compensate for brain shift but its use can lengthen the procedure. While brain shift has been recognized as a possible source of inaccuracy in DBS surgery, no comprehensive study has been reported that quantitatively analyzed brain deformation during this type of surgery. We studied nine movement disorder patients that underwent DBS surgery and measured their brain shift using a 3D non-rigid registration algorithm. Pre-op 3D MRI scans were first aligned rigidly with the corresponding post-operative (post-op) 3D MRI scans, which was followed with non-rigid registration. Brain shift vector field was generated over the entire brain and analyzed at selected points around the midbrain.

2. METHODS

2.1. MRI Acquisition Protocol

Pre-op and post-op T1 weighted MR images of nine patients that underwent DBS surgery were used for brain shift analysis. The Fast Field Echo protocol with gradient echo (flip angle = 30°, repetition time TR = 25 ms and echo time TE = 4.6 ms) was used to acquire both the pre-op and the post-op scans (200 slices of 256 x 256 pixels with in-plane resolution of 1 mm and slice thickness of 0.9 mm) on a Philips Medical System Gyroscan 1.5T MRI scanner.

2.2. Image Registration

Image registration was performed in two steps. The first step was to align the 3D pre-op and post-op images rigidly. We used the diploë for 3D rigid registration instead of using the whole head. The diploë is a spongy, porous, bony tissue between the hard outer and inner bone layers of the skull (Fig. 1). Since the diploë is rigid, the rigid registration based on the diploë is not affected by the brain tissue deformation. Furthermore, the diploë can be segmented as opposed to the entire skull bone whose boundaries are not clearly defined in T1 weighted MR images. Checkerboard displays* of the pre-op and the registered post-op images are shown in Fig. 2 for the case of whole head and diploë only 3D rigid registration. Once the skull was rigidly aligned, we ran a 3D non-rigid registration algorithm over the brain tissue that provided the brain shift vector field.

Thin plate splines[16] (TPS) were used to define the non-rigid transformation from the pre-op image to the post-op image. TPS parameters were computed using a set of corresponding nodes in each image and these

*Checkerboard display is a visualization technique that shows alternate square regions from two images.

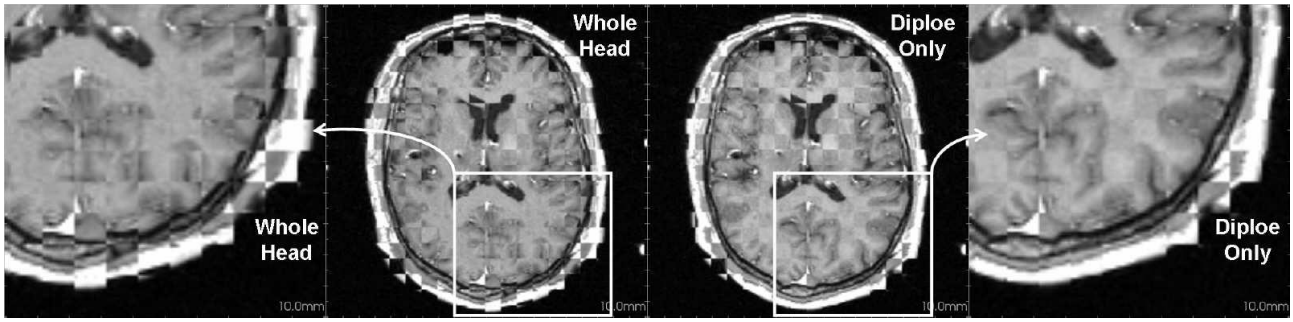

Figure 2. Axial checkerboard slices of a subject with the whole head and the diploë only rigid registration. The outer images are the zoomed in parts of the inner images showing improvement in the alignment of the diploë/skull using the diploë only registration as compared to the whole head registration.

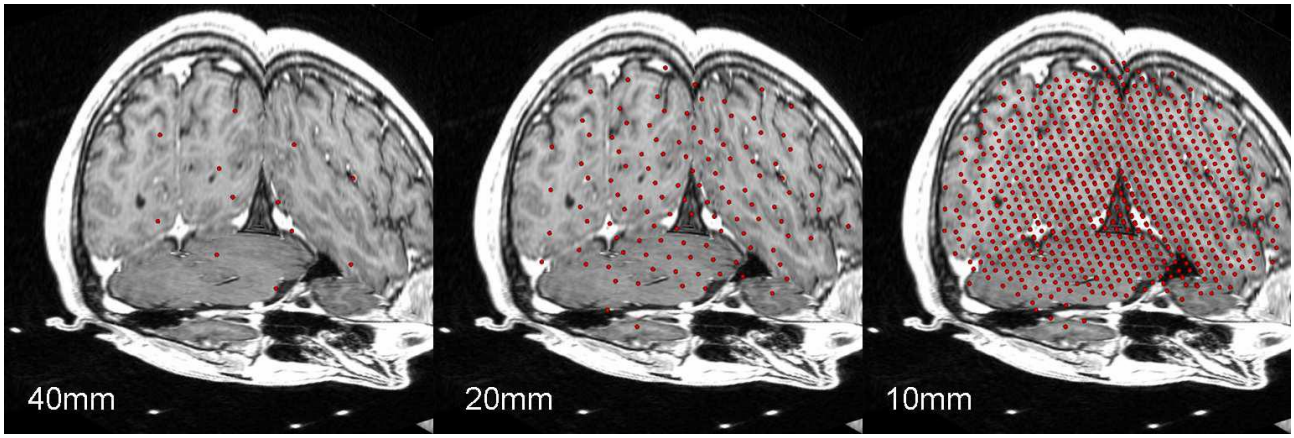

Figure 3. Control points for non-rigid registration at three resolution levels (40 mm, 20 mm and 10 mm) in the 3D view of the pre-op image.

parameters defined the TPS transformation between the two images. We used normalized mutual information[17] (NMI) as the image similarity measure between the pre-op and the post-op images. NMI between images I and J is:

$$NMI(I,J) = \frac{\sum_{i_a \epsilon I(X)} P(i_a)\log(P(i_a)) + \sum_{j_b \epsilon J(X)} P(j_b)\log(P(j_b))}{\sum_{(i_a,j_b)\epsilon I(X)\times J(X)} P(i_a,j_b)\log(P(i_a,j_b))}, \quad (1)$$

where X is the region of overlap of the two images, $I(X)$ and $J(X)$ are the sets of intensities of images I and J respectively, $P(i_a)$ and $P(j_b)$ are the marginal probabilities and $P(i_a, j_b)$ is the joint probability.

A multi-resolution approach was adopted in the implementation of the non-rigid registration algorithm with three resolutions of 40 mm, 20 mm and 10 mm of node spacing as shown in Fig. 3. A grid of nodes with 40 mm spacing (as shown in the left most image of Fig. 3) was placed over the segmented brain image at the lowest resolution level. The corresponding nodes in the post-op image were initially set using the transformation obtained by the rigid registration. The optimization was done using the Powell's method[18] for moving the nodes in order to maximize NMI at each resolution. The iterative maximization of NMI yields the final transformation

$$T = \arg\max_{T} NMI(I, J(T)). \quad (2)$$

T is the TPS transformation from the pre-op to the post-op image. Once a maximum of NMI was achieved at a given resolution, the node spacing was reduced to move to a higher resolution and the optimization procedure

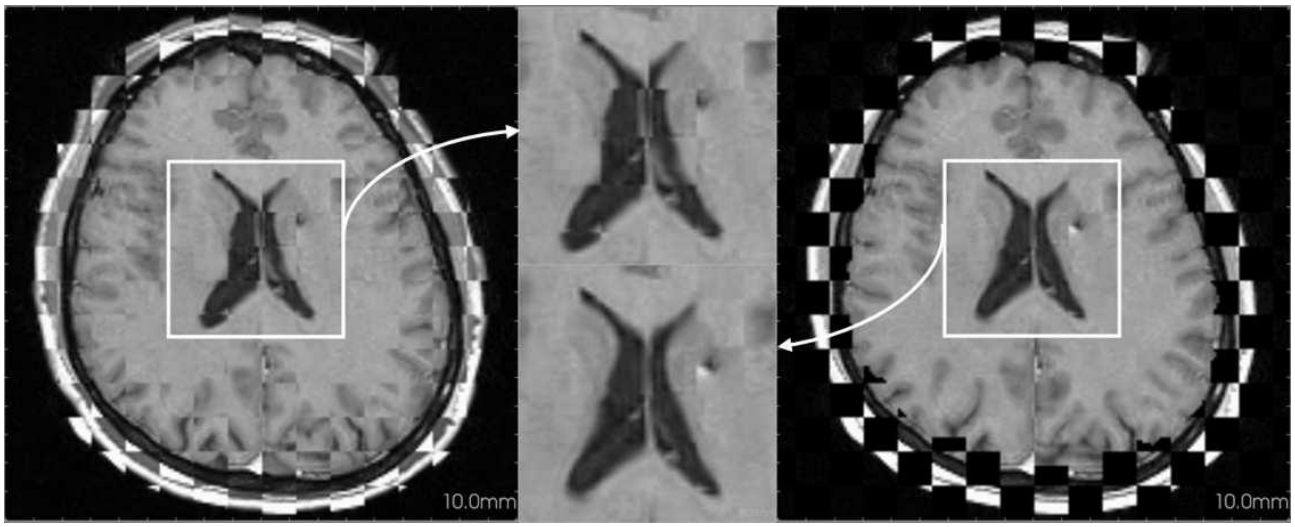

Figure 4. Axial checkerboard images of a subject. The leftmost image is after the rigid registration and the rightmost image is after the non-rigid registration. The center images are zoomed in lateral ventricle portions of the two images. Note the improvement of the ventricular wall alignment of the non-rigid registration over the rigid registration.

was repeated. The TPS parameters corresponding to the maximal NMI at the highest resolution were used to compute the brain shift vectors over the segmented brain region. Fig. 4 shows the registration results before and after non-rigid registration.

2.3. Brain Shift Analysis

Brain shift was analyzed using the brain shift vector field computed over the segmented brain using the non-rigid registration algorithm. The brain shift vector field of a subject is shown in Fig. 5. Brain shift vectors were also recorded at anterior commissure (AC), posterior commissure (PC), corner of the left putamen (PL) and corner of the right putamen (PR). The reason for selecting these four points (AC, PC, PL and PR) is that they are easily identifiable in T1 weighted MR images and they encompass the midbrain, which is the region of interest for the DBS surgery. These four points were manually marked for each subject (as shown in Fig. 8) and the brain shift at these points was computed using the non-rigid registration.

2.4. Evaluation

We assessed the performance of the algorithm by visual inspection of the diploë alignment for the rigid registration and alignment of brain structures (gyri, sulci, ventricles, putamena, etc) for the non-rigid registration using checkerboard and edge overlap displays. Misalignment, if present, can be seen at the boundaries of the square checkerboard regions. We mapped the edges of the post-op image over the edges of the pre-op image, which allowed any misalignment to be visible as a shift or mismatch of the edges.

3. RESULTS AND DISCUSSION

The pre-op image and the non-rigidly registered post-op image were visually compared in order to evaluate the quality of the registration algorithm. The checkerboard display of the non-rigidly registered pre-op and post-op images shows a better alignment than the checkerboard display of the rigidly registered pre-op and post-op images, as shown in Fig. 6. It can be seen in the top row images of Fig. 6 that the diploë was well aligned but the lateral ventricles were misaligned after the rigid registration. After the non-rigid registration (bottom row images of Fig. 6), the lateral ventricles as well as other structures were well aligned. Fig. 7 shows the edges of the pre-op image and the post-op image displayed over the pre-op image after the registration. It can be seen that the edges are close but still misaligned in the brain region after the rigid registration (left image of Fig. 7) especially in the inner structures. In the case of non-rigid registration (right image of Fig. 7), edges were well

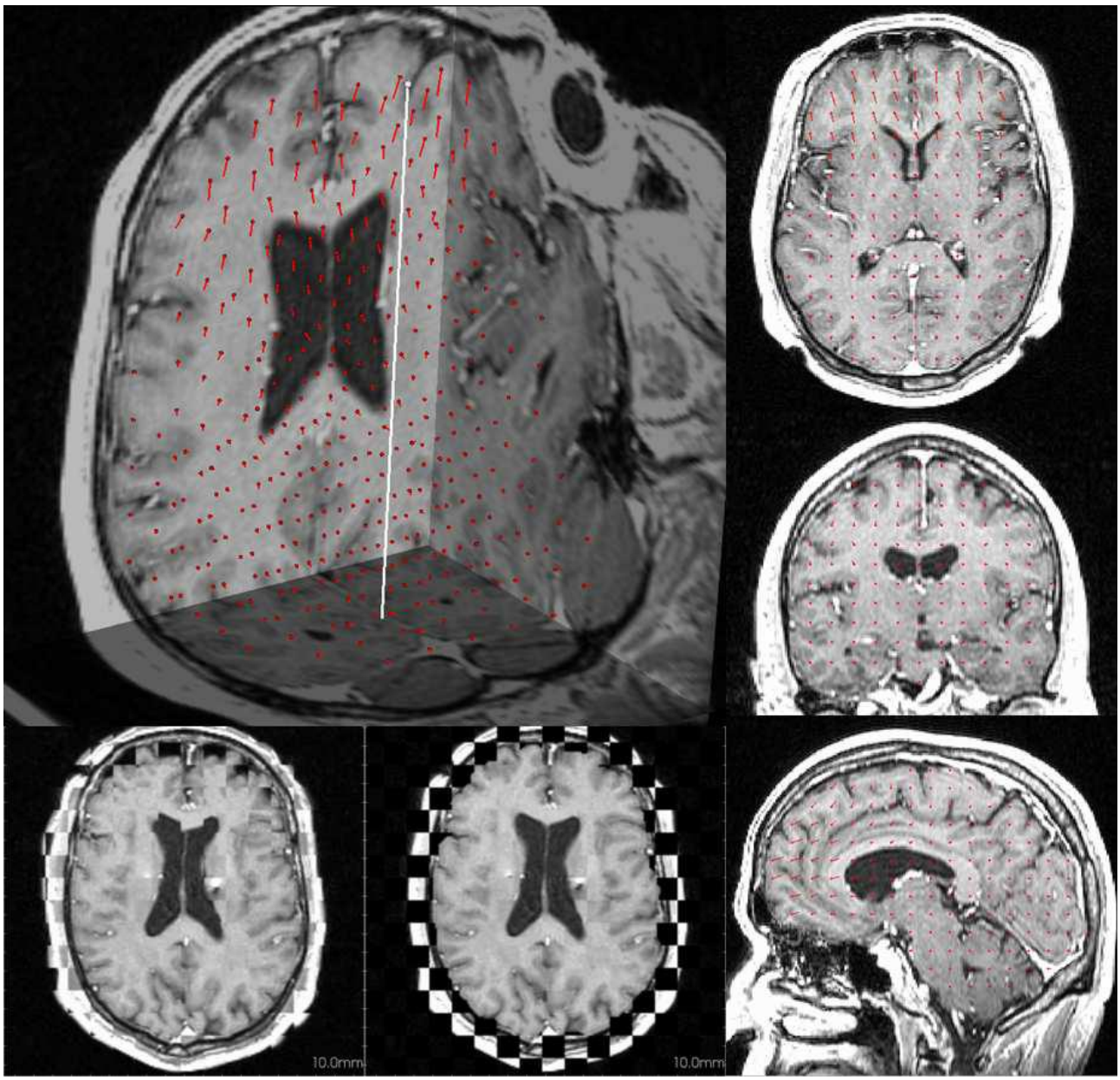

Figure 5. Vector field plot of brain shift vectors for one of the subjects shown on 3D preop image (top left image). Three images in the right column are axial, coronal and sagittal slices with the projections of the 3D shift vectors to the 2D slice. The white vector is the direction of gravity and red vectors are the shift vectors. Red dots in the 2D slices and red spheres in the 3D image represent the base of the shift vectors, whereas the lines show their length and direction. The bottom left image is the checkerboard image of the pre-op and the diploë-based rigidly registered post-op image whereas the bottom center image is the checkerboard image of the pre-op and the non-rigidly registered post-op image.

aligned for all the structures. Some edge differences were a consequence of the differences between the pre-op and the post-op images (e.g. implanted electrodes and leads).

The final TPS parameters were used to compute the brain shift vectors from the rigidly registered post-op image to the non-rigidly registered post-op image. The maximal brain shift was 8.3 mm for one of the subjects and the average maximal shift was 5 mm for the nine subjects. Statistical parameters of brain shift vectors measured over the whole brain are given in Table 1. Fig. 8 shows the maximum and the mean of the brain shift

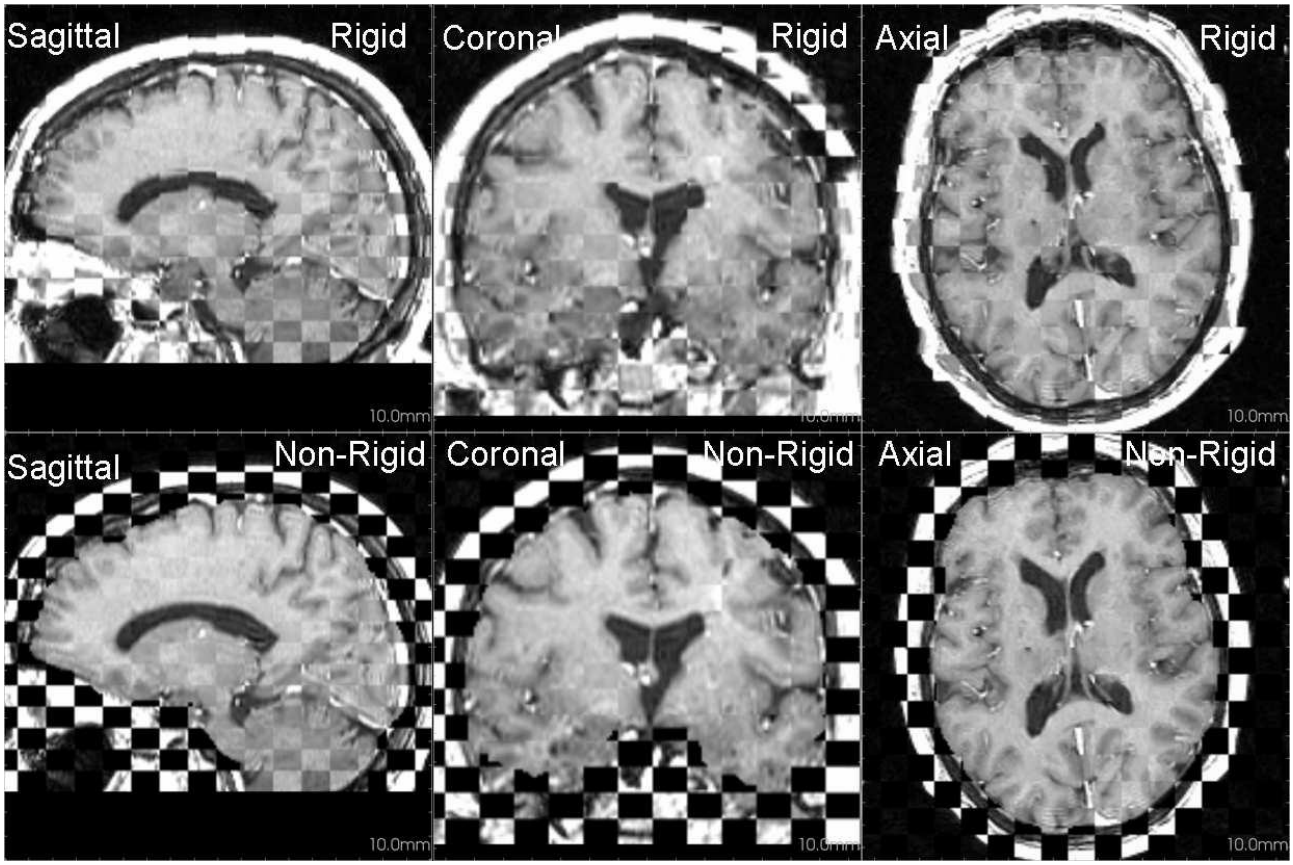

Figure 6. Sagittal, coronal and axial checkerboard displays of the pre-op and the post-op images after rigid and non-rigid registration. Top row shows the results after rigid registration whereas bottom row shows the results after non-rigid registration.

vectors recorded at AC, PC, PL and PR points for the nine subjects. Five subjects had at least a 1.5 mm shift in one or more of the four recorded points. This brain shift of at least 1.5 mm in more than half of the subjects is non-negligible given that the DBS targets are only a few millimeters in size (STN is approximately 4x6 mm and GPi has a radius of approximately 4 mm).

The anterior/superior parts of the brain experienced more shift as compared to posterior/inferior parts. This observation is further strengthened in Fig. 5, which shows that brain shifted more in anterior/superior regions than in the posterior/inferior regions. We also observed that brain shift vectors were mainly in the direction of gravity.

Fig. 9 shows the histograms of the AC, PC, PL and PR brain shift vectors for the nine subjects. Typically the shift was maximal in the putamen points, then AC and then PC. This may be explained by the fact that putamens were lateral and anterior to AC which in turn was anterior to PC, and the gravity vector was in the anterior-posterior direction. Thus, the deeper structures experienced less shift as compared to the anterior and outer structures.

4. CONCLUSIONS

A brain shift analysis was done on nine subjects that underwent DBS surgery. The pre-op and the post-op images were aligned using a 3D non-rigid registration algorithm. The maximal brain shift of 8.3 mm was recorded in one of the subjects and the average maximal shift was 5 mm for the nine subjects. It was observed that the

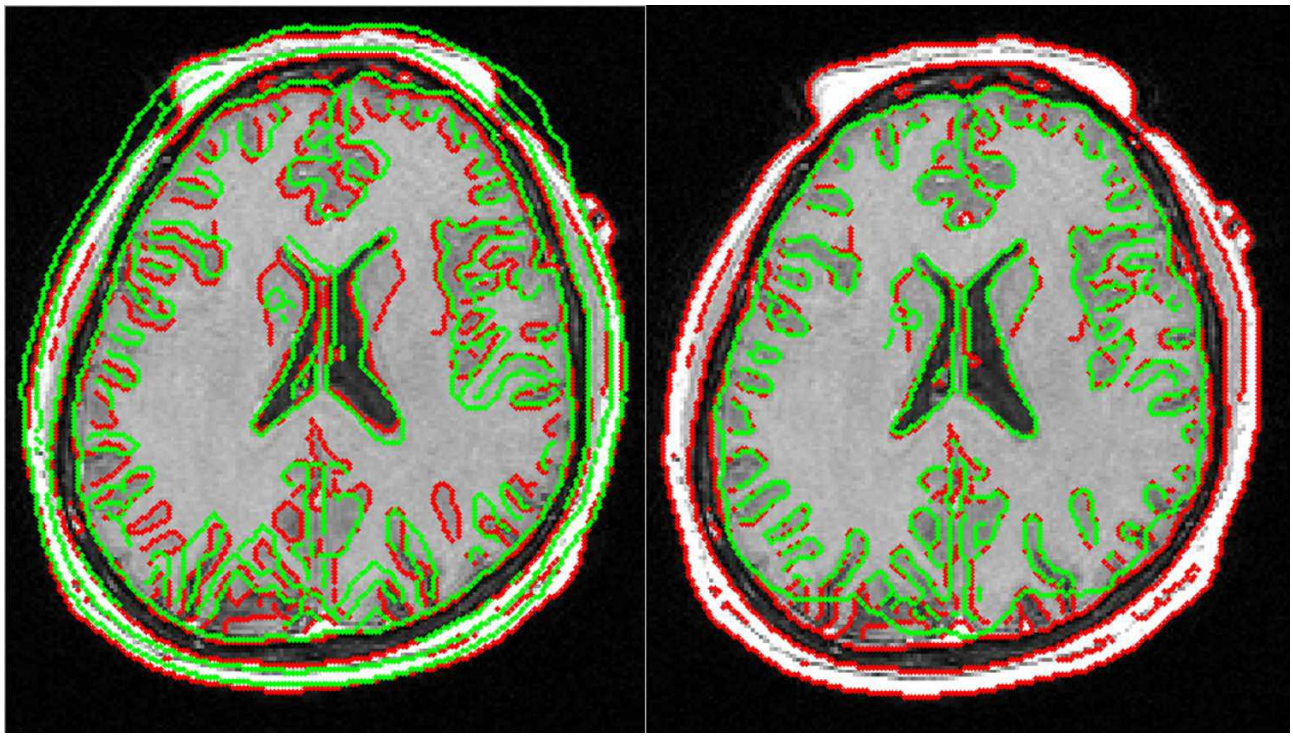

Figure 7. Edges of the pre-op image (red) and the post-op image (green) overlaid on the preop image after the registration for one of the subjects. The left image is after rigid registration whereas the right image is after non-rigid registration. A clear improvement in the edge alignment is visible for the non-rigid registration over the rigid registration. The non-rigid registration was performed over the brain tissue and this is why the green edges are not shown over the skull and scalp in the right image.

Table 1. Maximum, mean and standard deviation of the magnitude of the brain shift vectors.

Subject Number	Maximum Shift [mm]	Mean Shift [mm]	Standard Deviation [mm]
1	8.2	1.6	1.4
2	4.6	2.4	0.5
3	2.9	0.9	0.4
4	4.2	0.8	0.5
5	4.8	0.9	0.6
6	8.3	1.8	1.4
7	3.2	1	0.5
8	3	1	0.4
9	5.8	1	0.8

anterior/superior regions experienced more shift than the posterior/inferior regions and that the brain shift vectors were mainly in the direction of gravity. The magnitude of the recorded brain shift is comparable to the size of the DBS targets and therefore it should not be ignored.

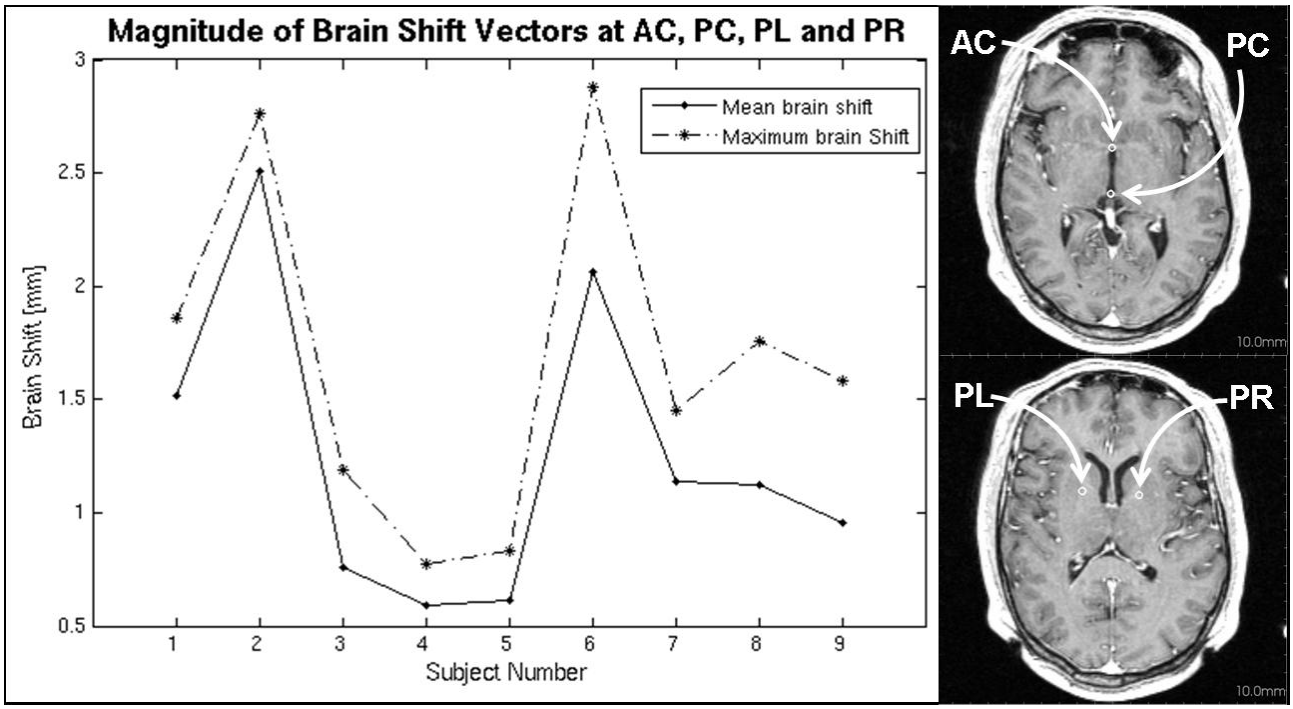

Figure 8. Maximum and mean magnitudes of the brain shift vectors recorded at AC, PC, PL and PR points after non-rigid registration (left graph). Right column shows the locations at which the AC, PC, PL and PR points are recorded manually in the axial slices of a pre-op image for one of the subjects.

REFERENCES

1. Byrd, D.L., et al. 2000. Deep brain stimulation for advanced Parkinson's disease. A.O.R.N. Journal 72(3), 387-90.
2. Honey, C., et al. 1999. New developments in the surgery for Parkinson's disease. Canadian Journal of Neurological Sciences 26 Suppl. 2, 45-52.
3. Starr, P.A., et al. 1998. Ablative surgery and deep brain stimulation for Parkinson's disease. Neurosurgery 43(5), 989-1013.
4. Gross, R.E., Lozano, A.M., 2000. Advances in neurostimulation for movement disorders. Neurological Research 22(3), 247-258.
5. Limousin, P., Krack, P., Pollak, P., Benazzouz, A., Ardouin, C., Hoffmann, D., Benabid, AL, 1998. Electrical stimulation of the subthalamic nucleus in advanced Parkinson's disease. N. Engl. J. Med. 15, 339(16), 1105-1111.
6. Atlas of Pathophysiology 2002. Anatomical Chart Company, Springhouse, PA.
7. Vitek, J.L., 1998. Surgery for dystonia. Neurosurgery Clinics of North America 9(2), 345-366.
8. Vitek, J.L., et al. 1998. Microelectrode-guided pallidotomy: technical approach and its application in medically intractable Parkinson's disease. J. Neurosurg. 88, 1027-1043.
9. Vitek, J.L., et al. 1999. Neuronal Activity in the Basal Ganglia in Patients with Generalized Dystonia and Hemiballismus. Annals of Neurosurgery 46(1), 22-35.
10. Hristova, A., et al. 2000. Effect and time course of deep brain stimulation of the globus pallidus and subthalamus on motor features of Parkinson's disease. Clinical Neuropharmacology 23(4), 208-211.
11. Rodrigez-Oroz, M.C., et al. 2001. The subthalamic nucleus in Parkinson's disease: somatotopic organization and physiological characteristics. Brain 124, 1777-1790.
12. Pollo, C., Meuli, R., Maeder, P., Vingerhoets, F., Ghika, J., Villemure, J.,2003. Subthalamic Nucleus Deep Brain Stimulation for Parkinsons Disease: Magnetic Resonance Imaging Targeting Using Visible Anatomical Landmarks. Proc. of the Meeting of the American Society for Stereotactic and Functional Surgery 80, 1-4.

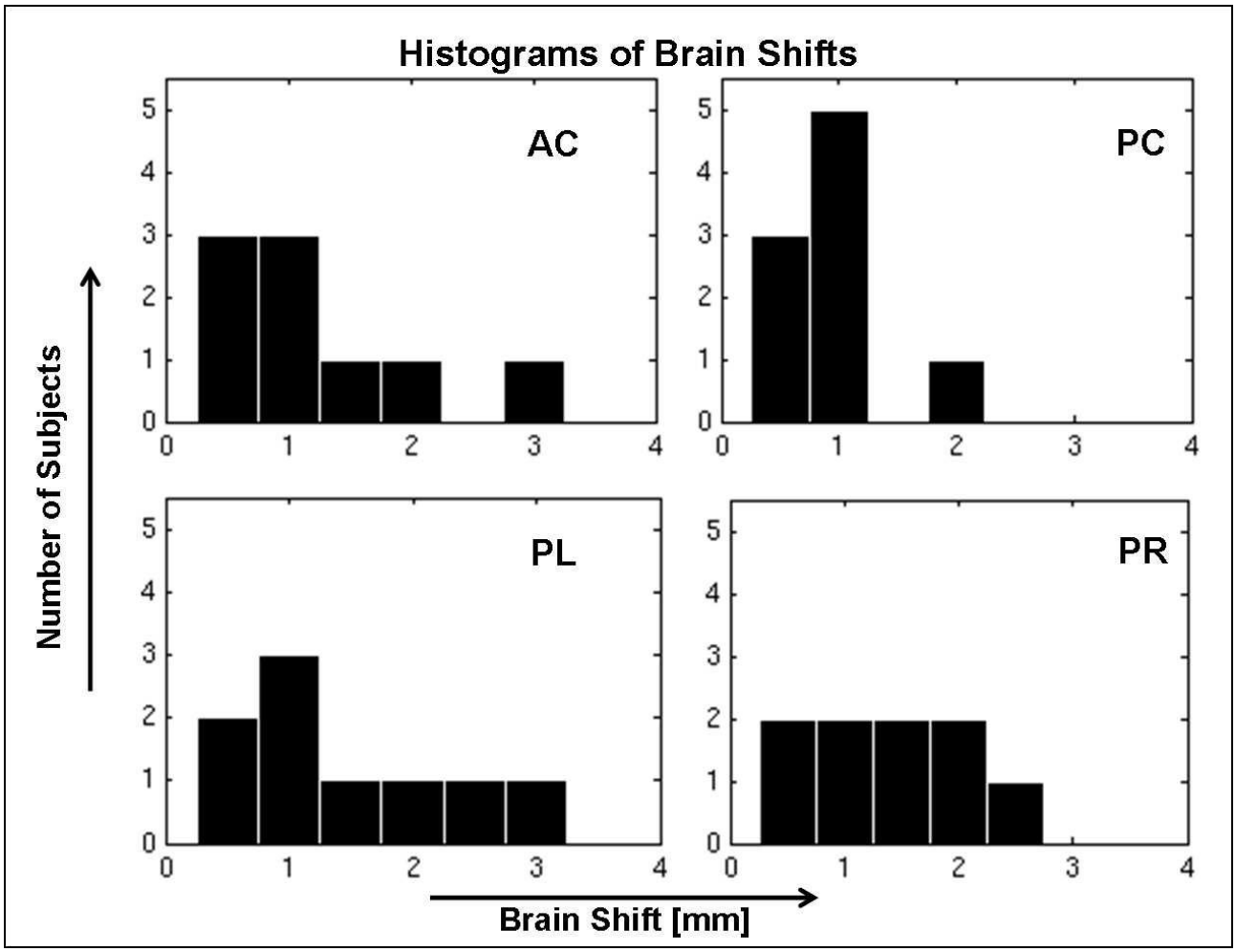

Figure 9. Histograms of the magnitudes of the brain shift vectors recorded at AC, PC, PL and PR after the non-rigid registration for the nine subjects.

13. Aziz, T.Z., Nandi, D., Parkin, S., Liu, X., Giladi, N., Bain, P., Gregory, R.G., Joint, C., Scott, R.B., Stein, J.F. 2001. Targeting the subthalamic nucleus. Stereotact Funct. Neurosurg. 77(1-4), 87-90.
14. Winkler, D., Tittgemeyer, M., Schwarz, J., Preul, C., Streckerk, K., Meixensberger, J., 2005. The first evaluation of brain shift during functional neurosurgery by deformation field analysis. J. Neurol. Neurosurg. Psychiatry 76, 1161-1163.
15. M.F. Khan, et-al. 2006. Brain shift analysis for deep brain stimulation surgery. IEEE International Symposium on Biomedical Imaging (ISBI), 654-657.
16. Bookstein, F. L., 1989. Principal Warps: Thin Plate Splines and the Decomposition of Deformations. IEEE Trans. Pattern Anal. Mach. Intell. 11, 567-585.
17. C. Studholme, et-al. 1999. An Overlap Invariant Entropy Measure of 3D Medical Image Alignment. Pattern Recognition, 32, 71-86.
18. Press W., Flannery B., Teukolsky S., Vetterling W. 1992. Numerical Recipes in C: The Art of Scientific Computing. 2nd ed. Cambrige Univeristy Press.